Journal of Power Sources 254 (2014) 106–111

Contents lists available at ScienceDirect

Journal of Power Sources

journal homepage: www.elsevier.com/locate/jpowsour

Sb_2O_3-modified $LiNi_{1/3}Co_{1/3}Mn_{1/3}O_2$ material with enhanced thermal safety and electrochemical property

Zenghui Han [a], Jinpeng Yu [b], Hui Zhan [a,*], Xingjiang Liu [b], Yunhong Zhou [a]

[a] College of Chemistry and Molecular Sciences, Wuhan University, Wuhan 430 072, China
[b] National Key Laboratory of Power Source, Tianjin Institute of Power Sources, Tianjin 300 381, China

HIGHLIGHTS

- $Sb_2O_3/LiMO_2$ was obtained by rheological phase method and ball milling post-treatment.
- $Sb_2O_3/LiMO_2$ has enhanced cycling stability, rate capability, and thermal safety.
- $Sb_2O_3/LiMO_2$ electrodes have maintained good kinetic property and improved interface.
- Sb_2O_3-coated separator maybe has similar positive effect as $Sb_2O_3/LiMO_2$.

ARTICLE INFO

Article history:
Received 5 October 2013
Accepted 29 November 2013
Available online 24 December 2013

Keywords:
Layered material
Antimony oxide
Lithium ion battery
Electrochemical performance
Thermal safety

ABSTRACT

The layered $LiMO_2$ (M = Ni, Co and Mn) materials $LiNi_{1/3}Co_{1/3}Mn_{1/3}O_2$ and $LiNi_{0.4}Co_{0.2}Mn_{0.4}O_2$ are synthesized by rheological phase method. Sb_2O_3-modified phases are further obtained by mechanical ball milling treatment. The structure and morphology of the bare and modified samples are characterized by X-ray diffraction, scanning electron microscopy and transmission electron microscopy. Charge/discharge tests indicate that the modified phases all improve cycling stability, rate capability and thermal safety. Careful comparison of the charge/discharge profiles reveals that the serious polarization increment in cycling is suppressed in the Sb_2O_3-modified $LiMO_2$ electrodes. AC impedance shows that $Sb_2O_3/LiNi_{1/3}Co_{1/3}Mn_{1/3}O_2$ electrode has smaller R_{ct} and R_f value. Further analysis proves that Sb_2O_3 hinders the reaction between electrolyte and cathode during charge/discharge process and helps to stabilize the SEI. Other experiments prove that using Sb_2O_3-coated separator can achieve similar positive effect on layered $LiMO_2$ cathode.

1. Introduction

Nowadays, Li-ion battery (LIB) has been widely investigated for transportation applications, such as hybrid electric vehicle (HEV), electric vehicle (EV) and plug-in hybrid electric vehicle (PHEV) because of its high energy density. However, in current LIB technology, the energy density and the power density are both mainly determined by the cathode material [1,2]. Though the conventional $LiCoO_2$ has already achieved a great success in LIB market, its safety and cost are always the big issues when large-scale application is required. The layered $LiMO_2$ (M = Ni, Co and Mn), such as $LiNi_{1/3}Co_{1/3}Mn_{1/3}O_2$ [3], has been of great interests as one of the most promising alternative materials for $LiCoO_2$ in lithium-ion battery due to the lower cost, less toxicity, higher reversible capacity and milder safety characteristics [4–7]. Layered $LiMO_2$ (M = Ni, Co and Mn) has the analogous structure with $LiCoO_2$. The combination of Ni, Mn and Co in $LiNi_{1/3}Co_{1/3}Mn_{1/3}O_2$ could provide higher initial discharge capacity of 215 mA h g^{-1} in the voltage range of 2.5–4.7 V [8]. However, its rate performance, cycling stability and thermal safety still need to be improved, especially when a higher upper voltage limit applies.

To improve the electrochemical property of the layered $LiMO_2$ (M = Ni, Co and Mn), the substitution of metal ions such as Mg^{2+} [9] and Y^{3+} [10] has been investigated. It is reported that partial cationic substitution for Ni^{2+} could stabilize the structure and reduce cation mixing. Additionally, He et al. [11] used Sn^{4+} to dope $LiNi_{3/8}Co_{2/8}Mn_{3/8}O_2$ for enhancing its rate capability. They think the bigger ionic radius of substitution will expand the pathway for Li^+ diffusion. Kam et al. [12] reported that partial substitution of Co^{3+} by Ti^{4+} in $LiNi_{1/3}Co_{1/3}Mn_{1/3}O_2$ could increase the discharging capacity and improve the cycling characteristic.

Another typical approach is surface treatment. Coating $LiMO_2$ phase with some stable or high-conductive materials has been

* Corresponding author, Tel: +86 27 68756931; fax: +86 27 68754067.
E-mail address: zhanhui3620@126.com (H. Zhan).

0378-7753/$ – see front matter © 2014 Elsevier B.V. All rights reserved.
http://dx.doi.org/10.1016/j.jpowsour.2013.11.126

proposed. Kweon et al. [13] have observed a better cycling property of Al_2O_3-coated $LiCoO_2$ at high cut-off. Other coating substances, such as Sb_2O_3 [14], C [15], CeO_2 [16], $AlPO_4$ [17] and ZrF_x [18], have been investigated and shown a certain extent of improvement. Generally, the improvement is ascribed to 1) restraining the side reactions between active material and electrolyte, 2) enhancing the surface conductivity, 3) limiting the oxygen vacancy. For instance, Park et al. [19] found that $LaPO_4$-coated $LiNi_{0.5}Co_{0.2}Mn_{0.3}O_2$ could suppress the dissolution of transition metals into electrolyte and prevent phase transformation during cycling. ZrO_2-modified $LiNi_{1/3}Co_{1/3}Mn_{1/3}O_2$ [20] was studied and showed an increased Li^+ diffusion coefficient and a reduced active energy of interfacial Li^+ transfer reaction.

Besides, morphology optimization or advanced processing method has been reported to achieve a good electrochemical performance. Sun et al. [21] synthesized the micro-scale spherical core-shell structure $Li[(Ni_{0.8}Co_{0.1}Mn_{0.1})_{0.8}(Ni_{0.5}Mn_{0.5})_{0.2}]O_2$ to get high initial discharge capacity (188 mA h g^{-1}) and excellent thermal stability. Chen et al. [22] presented one-step synthesis of $LiNi_{1/3}Co_{1/3}Mn_{1/3}O_2$ by a radiation-assisted polymer-gel method to enhance the capacity retention and rate performance.

In this work, $Sb_2O_3/LiNi_{1/3}Co_{1/3}Mn_{1/3}O_2$ and $Sb_2O_3/LiNi_{0.4}Co_{0.2}Mn_{0.4}O_2$ composites were prepared by rheological phase method and ball-milling post-treatment. The structure and morphology of $LiNi_{1/3}Co_{1/3}Mn_{1/3}O_2$ and $LiNi_{0.4}Co_{0.2}Mn_{0.4}O_2$ with or without Sb_2O_3 modification were investigated. Meanwhile, their electrochemical properties and thermal safety were compared. It is found that the modified phases present improved thermal safety and much better electrochemical performance at higher upper voltage. AC impedance measurement reveals that the $Sb_2O_3/LiNi_{1/3}Co_{1/3}Mn_{1/3}O_2$ electrode can maintain a better electrochemical kinetics in cycling than the bare $LiNi_{1/3}Co_{1/3}Mn_{1/3}O_2$ electrode. Finally, the approach of using Sb_2O_3-coated separator is proposed and its positive effect has been verified by some experiments.

2. Experimental

The two samples, $LiNi_{1/3}Co_{1/3}Mn_{1/3}O_2$ and $LiNi_{0.4}Co_{0.2}Mn_{0.4}O_2$, were synthesized by rheological phase method. Stoichiometric amount of Li_2CO_3, $Ni(CH_3COO)_2{\cdot}4H_2O$, $Co(CH_3COO)_2{\cdot}4H_2O$, $Mn(CH_3COO)_2{\cdot}4H_2O$ and oxalic acid were mixed. And then a proper amount of water was added. After stirring the mixture at 80–90 °C for 4 h, it was dried at 120 °C for 10 h, followed by annealing at 850 °C for 20 h. The products were well ground prior to further use.

The Sb_2O_3-compostited materials were obtained by ball-milling the nano-sized Sb_2O_3 with the above-prepared layered material. The mass ratio of Sb_2O_3 and $LiNi_{1/3}Co_{1/3}Mn_{1/3}O_2$ (or $LiNi_{0.4}Co_{0.2}Mn_{0.4}O_2$) was 3:100.

Structure of the resulting materials was determined by the X-ray diffraction (XRD) method performing on a D_8-advance X-ray diffractometer (Bruker) with Cu Kα radiation ($\lambda = 0.15418$ nm) and 4° min^{-1} scan rate. Particle information of the prepared materials was obtained from scanning electron microscope measurement (SEM, Quanta-200). The TEM images were collected on a JEM-2100 transmission electron microscope under an accelerating voltage of 200 keV.

Charge/discharge experiments were carried out on a Land battery test system (China). The CR2016 coin cells were assembled in an argon-filled glove box (MB200B, M. Braun GmbH, Germany) with lithium anode and the cathode composing of 80 wt.% active material, 10 wt.% acetylene black and 10 wt.% polytetrafluoroethylene (PTFE) binder. The electrolyte was 1 mol L^{-1} $LiPF_6$ in a mixed solvent of ethylene carbonate (EC), dimethyl carbonate (DMC) and ethylene methyl carbonate (EMC) (1:1:1 by volume). The cells were cycled at 0.5 C (1 C = 200 mA g^{-1}) in the potential range of 3.0–4.3 V or 3.0–4.6 V.

Thermal safety of the bare material and the composite phase was evaluated on a differential scanning calorimeter (DSC, TA-Q200). The coin cells were galvanostatically charged to 4.7 V, and then kept at this potential for another 8 h. After detaching the cell in the Ar-filled glove box, the cathode was taken out, then placed in an Al crucible and subjected to DSC analysis. The DSC measurement was conducted in N_2 atmosphere from ambient temperature to 350 °C at a heating rate of 10 °C min^{-1}.

The AC impedance measurement was conducted on an Autolab Electrochemical Workstation (Autolab PGSTAT30, Eco Chemie) with a three-electrode cell, in which lithium foil worked as both the counter and the reference electrode. All the impedance data was recorded in a frequency range from 100 kHz to 0.01 Hz with voltage amplitude of 5 mV.

3. Results and discussion

Powder XRD patterns of the pristine layered materials and the composite phases are presented in Fig. 1. All the XRD plots are essentially the same except that the composite phases show the characteristic peak of Sb_2O_3. The diffraction peaks marked with "*" in the 2θ range of 25–30° should be ascribed to Sb_2O_3. Other characteristic peaks of Sb_2O_3 could not be observed because of the low concentration of Sb_2O_3. All the diffraction lines of the bare samples can be indexed by a hexagonal α-$NaFeO_2$ type structure (space group $R\bar{3}m$). Moreover, the distinct splitting of (006)/(102) and (108)/(110) indicates the well-developed layered structure.

Scanning electron microscopy (SEM) images of $LiNi_{1/3}Co_{1/3}Mn_{1/3}O_2$ and $Sb_2O_3/LiNi_{1/3}Co_{1/3}Mn_{1/3}O_2$ composite are given in Fig. 2a and b. It is clearly seen that the particle size of $LiNi_{1/3}Co_{1/3}Mn_{1/3}O_2$ is within sub-microns and the surface of particle is smooth. The SEM image of $Sb_2O_3/LiNi_{1/3}Co_{1/3}Mn_{1/3}O_2$ composite does not show significant difference from that of $LiNi_{1/3}Co_{1/3}Mn_{1/3}O_2$. The composite mostly preserves the morphology of $LiNi_{1/3}Co_{1/3}Mn_{1/3}O_2$ phase. The TEM images of $LiNi_{1/3}Co_{1/3}Mn_{1/3}O_2$ (Fig. 2c) and Sb_2O_3 (Fig. 2d) indicate that the particle size of $LiNi_{1/3}Co_{1/3}Mn_{1/3}O_2$ is about 200–400 nm, and Sb_2O_3 has a round shape with 50–200 nm size. From the TEM image of $Sb_2O_3/LiNi_{1/3}Co_{1/3}Mn_{1/3}O_2$ composite (Fig. 2e), it can be observed that the small Sb_2O_3 particles adhere to the surface of $LiNi_{1/3}Co_{1/3}Mn_{1/3}O_2$.

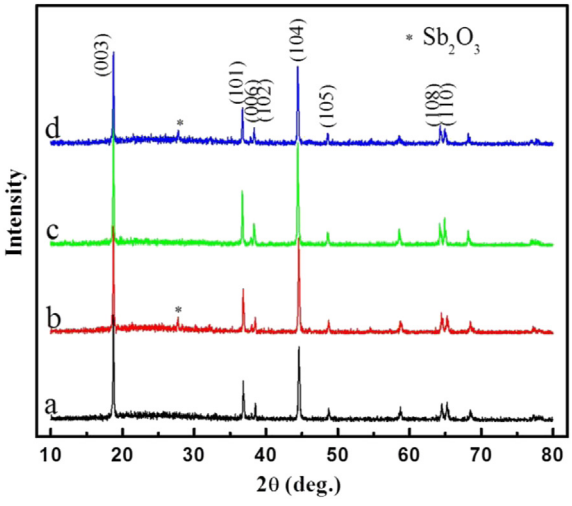

Fig. 1. XRD patterns of all the resulting samples (a) $LiNi_{1/3}Co_{1/3}Mn_{1/3}O_2$, (b) $Sb_2O_3/LiNi_{1/3}Co_{1/3}Mn_{1/3}O_2$, (c) $LiNi_{0.4}Co_{0.2}Mn_{0.4}O_2$, (d) $Sb_2O_3/LiNi_{0.4}Co_{0.2}Mn_{0.4}O_2$.

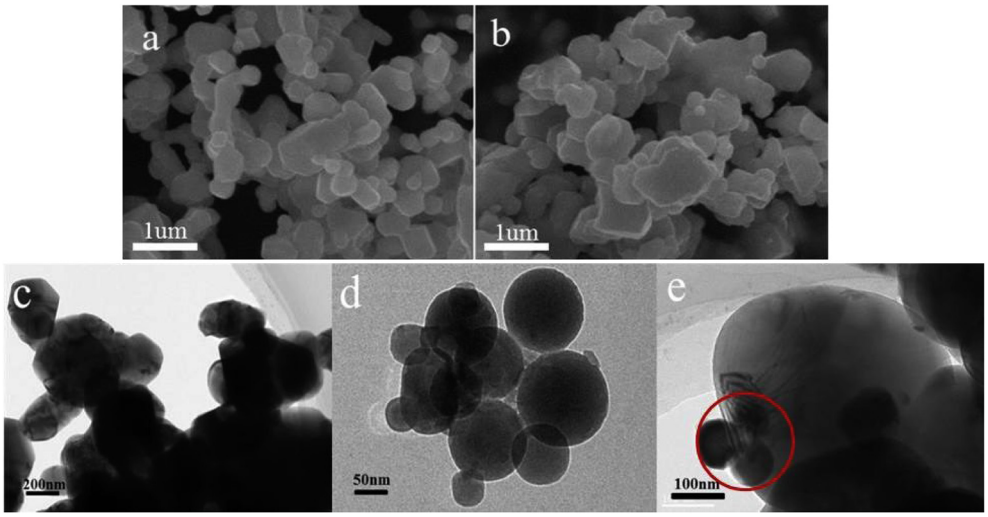

Fig. 2. SEM images of (a) $LiNi_{1/3}Co_{1/3}Mn_{1/3}O_2$, (b) $Sb_2O_3/LiNi_{1/3}Co_{1/3}Mn_{1/3}O_2$, and TEM images of (c) $LiNi_{1/3}Co_{1/3}Mn_{1/3}O_2$, (d) Sb_2O_3, (e) $Sb_2O_3/LiNi_{1/3}Co_{1/3}Mn_{1/3}O_2$.

Fig. 3 shows the charge/discharge curves of $LiNi_{1/3}Co_{1/3}Mn_{1/3}O_2$ and $Sb_2O_3/LiNi_{1/3}Co_{1/3}Mn_{1/3}O_2$. When the electrodes were cycled in the voltage range of 3.0–4.3 V, as shown in Fig. 3a, their charge/discharge curves are quite similar either in the 1st cycle or in the 51st cycle. When the voltage range is extended to 3–4.6 V (Fig. 3b), their initial charge/discharge profiles are still similar except that the composite capacity shows a little bit lower than the bare capacity due to the presence of inert Sb_2O_3 component. However, in the 51st cycle, the discharging voltage of bare $LiNi_{1/3}Co_{1/3}Mn_{1/3}O_2$ declines much more than that of the composite phase. Besides, the much larger hysteresis between the charging and discharging plateau of $LiNi_{1/3}Co_{1/3}Mn_{1/3}O_2$ than $Sb_2O_3/LiNi_{1/3}Co_{1/3}Mn_{1/3}O_2$ composite indicates a more significant polarization increment in the former phase. Obviously, the Sb_2O_3 component in $Sb_2O_3/LiNi_{1/}$

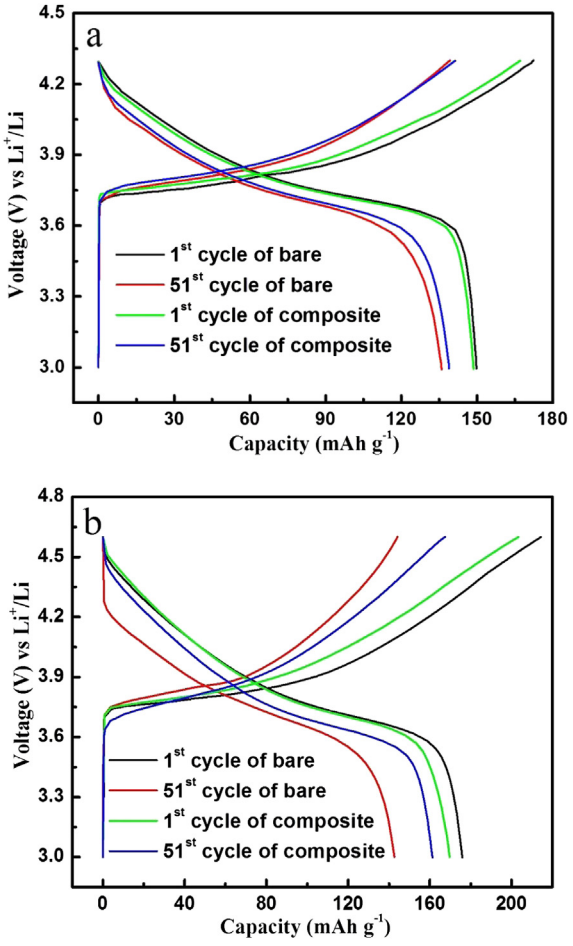

Fig. 3. Charge/discharge curves of $LiNi_{1/3}Co_{1/3}Mn_{1/3}O_2$ and $Sb_2O_3/LiNi_{1/3}Co_{1/3}Mn_{1/3}O_2$ at the current density of 100 mA g^{-1} in (a) 3–4.3 V and (b) 3–4.6 V.

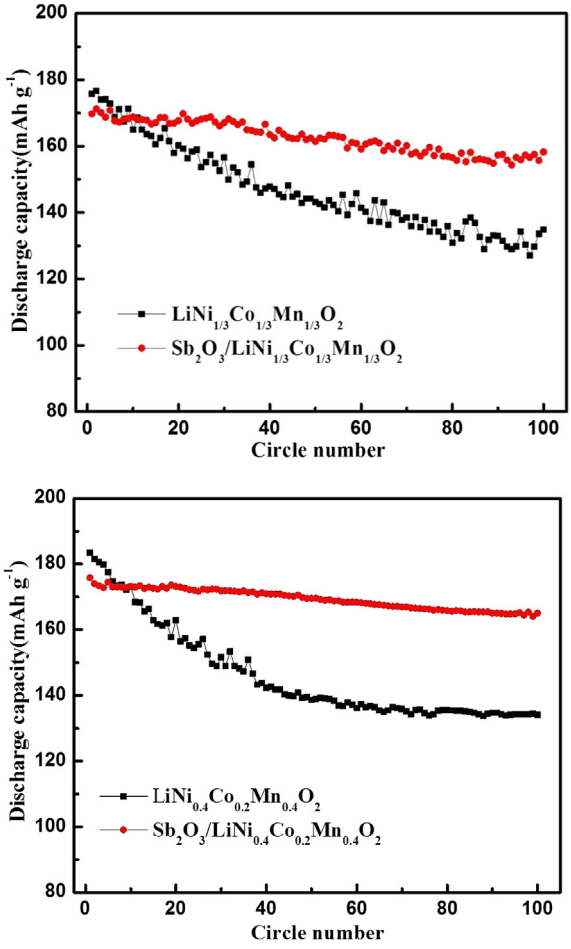

Fig. 4. Discharge capacity vs. Cycle number of all resulted samples in 3.0–4.6 V at the current density of 100 mA g^{-1}.

$_3Co_{1/3}Mn_{1/3}O_2$ composite is able to reduce the polarization and improve the electrochemical performance especially when high voltage applies.

Fig. 4 compares the cycling properties of bare and Sb_2O_3-composited $LiNi_{1/3}Co_{1/3}Mn_{1/3}O_2$ and $LiNi_{0.4}Co_{0.2}Mn_{0.4}O_2$ at the current of 100 mA g^{-1} between 3.0 and 4.6 V. Capacity loss of bare sample is very obvious, while the capacity loss is greatly suppressed after compositing with Sb_2O_3. Capacity retention increases from 73.5% for bare $LiNi_{1/3}Co_{1/3}Mn_{1/3}O_2$ to 91.4% for $Sb_2O_3/LiNi_{1/3}Co_{1/3}Mn_{1/3}O_2$, and the capacity retention is boosted from 73.3% for $LiNi_{0.4}Co_{0.2}Mn_{0.4}O_2$ to 93.8% for $Sb_2O_3/LiNi_{0.4}Co_{0.2}Mn_{0.4}O_2$. The results show that after composited with Sb_2O_3, the cycling performance of the layered compounds has been enhanced significantly.

The discharge capacity of bare and Sb_2O_3-modified $LiNi_{1/3}Co_{1/3}Mn_{1/3}O_2$ and $LiNi_{0.4}Co_{0.2}Mn_{0.4}O_2$ at various current is shown in Fig. 5. The cells were charged and discharged between 3.0 V and 4.6 V at the 0.2 C, 0.5 C, 1 C, 2 C and 4 C every 10 cycles. With the increasing current, the discharging capacity of the bare phases drops quickly, while the modified phases show much better capacity retention. For instance, $Sb_2O_3/LiNi_{1/3}Co_{1/3}Mn_{1/3}O_2$ delivered a capacity of ~135 mA h g^{-1} at 4 C while bare $LiNi_{1/3}Co_{1/3}Mn_{1/3}O_2$ only had a capacity of ~72 mA h g^{-1} at 4 C rate. The significant improvement can also be observed on $Sb_2O_3/LiNi_{0.4}Co_{0.2}Mn_{0.4}O_2$, which presented a 120% capacity increase at 4 C comparing with the bare $LiNi_{1/3}Co_{1/3}Mn_{1/3}O_2$ at 4 C. The results shown in Fig. 5 clearly indicate the improved rate capability of the Sb_2O_3-modified layered compounds. Suppression of the polarization increment should be used to explain the improvement as being mentioned above. To better understand the reason, AC impedance measurements were done and the results are shown in Fig. 6. Fig. 6a presents the Nyquist plots of the fresh $LiNi_{1/3}Co_{1/3}Mn_{1/3}O_2$ and $Sb_2O_3/LiNi_{1/3}Co_{1/3}Mn_{1/3}O_2$ electrode. A semicircle in the high frequency range representing charge transfer resistance (R_{ct}) and a sloping line at low frequency representing Warburg resistance can be observed in both the electrodes. $Sb_2O_3/LiNi_{1/3}Co_{1/3}Mn_{1/3}O_2$ electrode showed a semicircle with notably smaller diameter comparing with $LiNi_{1/3}Co_{1/3}Mn_{1/3}O_2$ electrode. In Fig. 6b, AC impedance plots of the cycled electrodes are displayed. The bare and the modified phase both present a new semicircle in the high frequency range (representing R_f), suggesting the SEI information after repeated charging/discharging. Aurbach et al. [23] reported that capacity fading of layered $LiCoO_2$ on cycling and storage at elevated temperature was attributed to the increase of surface film resistance. In our work, similar observation has been obtained. Besides, the diameter of the semicircle in high-to-medium frequency range representing R_{ct} is much larger in the cycled $LiNi_{1/3}Co_{1/3}Mn_{1/3}O_2$ electrode than that in the cycled $Sb_2O_3/LiNi_{1/3}Co_{1/3}Mn_{1/3}O_2$ electrode. The data in Table 1 compares the R_{ct} and R_f value of bare and modified phases. It can be seen that Sb_2O_3-modified $LiNi_{1/3}Co_{1/3}Mn_{1/3}O_2$ electrode has a much smaller R_{ct} value than $LiNi_{1/3}Co_{1/3}Mn_{1/3}O_2$ electrode. Meanwhile, after cycling

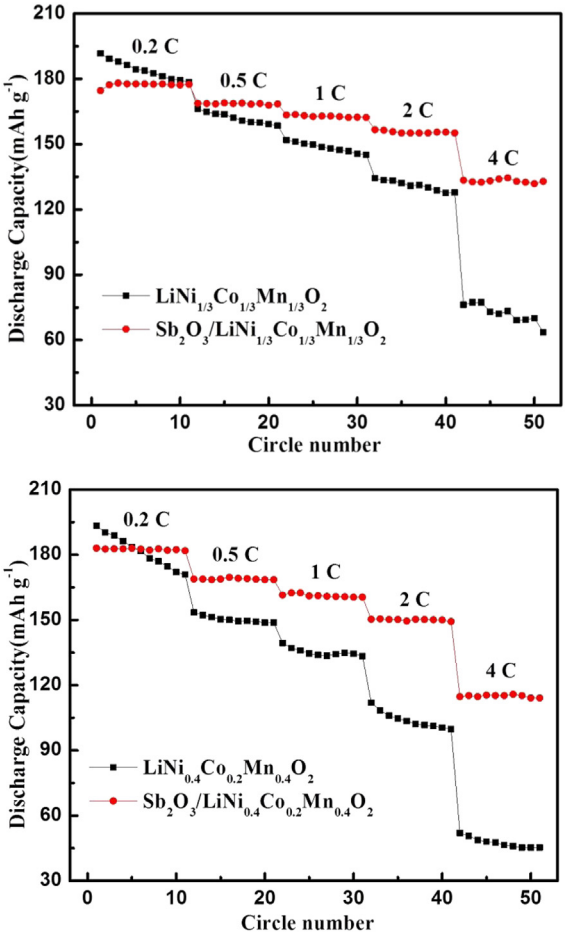

Fig. 5. Discharge profiles of bare and composited $LiNi_{1/3}Co_{1/3}Mn_{1/3}O_2$ and $LiNi_{0.4}Co_{0.2}Mn_{0.4}O_2$ at the various current between 3.0 V and 4.6 V.

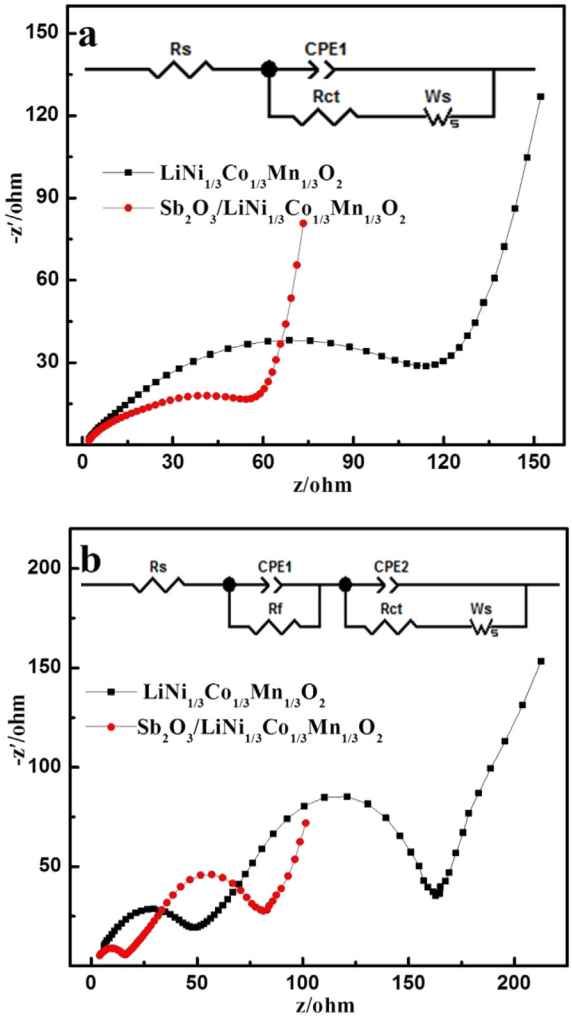

Fig. 6. AC impedance spectrums of bare and composited $LiNi_{1/3}Co_{1/3}Mn_{1/3}O_2$ (a) fresh electrodes and (b) cycled electrodes.

Table 1
AC impedance data of bare and modified $LiNi_{1/3}Co_{1/3}Mn_{1/3}O_2$ cathode.

		R_f (Ohm)	R_{ct} (Ohm)
$LiNi_{1/3}Co_{1/3}Mn_{1/3}O_2$	Fresh	–	140.0
$Sb_2O_3/LiNi_{1/3}Co_{1/3}Mn_{1/3}O_2$		–	54.7
$LiNi_{1/3}Co_{1/3}Mn_{1/3}O_2$	Cycled	53.5	118.3
$Sb_2O_3/LiNi_{1/3}Co_{1/3}Mn_{1/3}O_2$		16.3	77.0

R_f value of Sb_2O_3-modified $LiNi_{1/3}Co_{1/3}Mn_{1/3}O_2$ electrode is also smaller than that of $LiNi_{1/3}Co_{1/3}Mn_{1/3}O_2$ electrode. Therefore, the enhanced cycling stability and rate capability of Sb_2O_3 modified phases can be explained as the SEI and R_{ct} improvement due to the alleviation of side reactions between active material and electrolyte at high voltage as well as the better maintaining of the kinetic property.

Thermal stability of $LiNi_{1/3}Co_{1/3}Mn_{1/3}O_2$, $LiNi_{0.4}Co_{0.2}Mn_{0.4}O_2$ and their Sb_2O_3-modified phases has been evaluated by DSC in Fig. 7. $Sb_2O_3/LiMO_2$ ($LiMO_2$ = $LiNi_{1/3}Co_{1/3}Mn_{1/3}O_2$ or $LiNi_{0.4}Co_{0.2}Mn_{0.4}O_2$) can notably enhance the thermal safety. For $LiNi_{1/3}Co_{1/3}Mn_{1/3}O_2$, the exothermic reaction initiated at around 262 °C, but it was delayed to 295 °C in $Sb_2O_3/LiNi_{1/3}Co_{1/3}Mn_{1/3}O_2$ accompany with an obvious decrease in heat release. Comparing $LiNi_{0.4}Co_{0.2}Mn_{0.4}O_2$ with $Sb_2O_3/LiNi_{0.4}Co_{0.2}Mn_{0.4}O_2$, similar observation can be obtained. The stabilized interface should be the reason for the improvement in thermal safety.

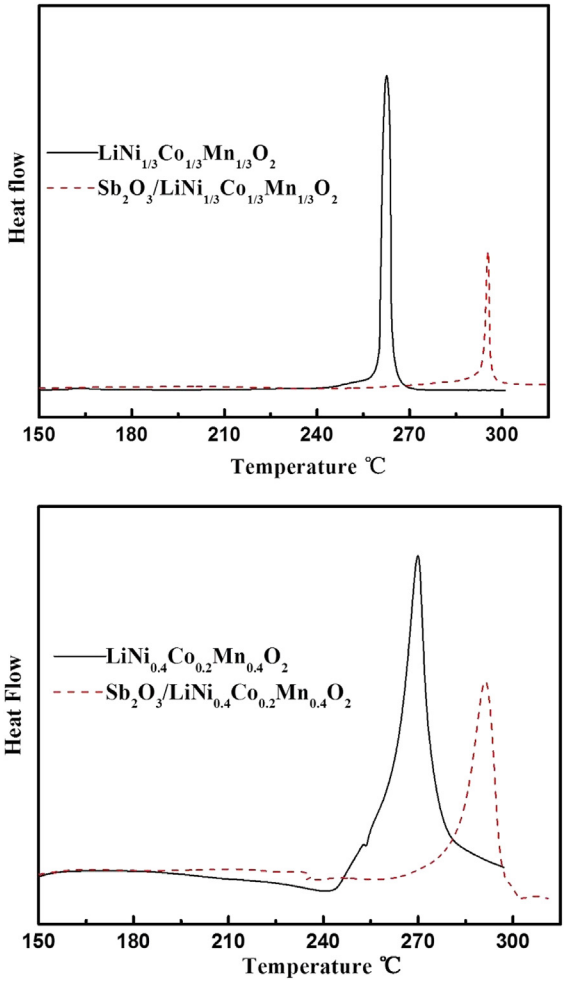

Fig. 7. DSC of bare and composite $LiNi_{1/3}Co_{1/3}Mn_{1/3}O_2$ and $LiNi_{0.4}Co_{0.2}Mn_{0.4}O_2$.

In the above discussion, the positive effect of Sb_2O_3 modification on the cycling stability, rate performance and thermal safety has been demonstrated. It has to be further pointed out that in the Sb_2O_3-modified phases, $Sb_2O_3/LiNi_{1/3}Co_{1/3}Mn_{1/3}O_2$ or $Sb_2O_3/LiNi_{0.4}Co_{0.2}Mn_{0.4}O_2$ composite have been obtained by simple ball milling, and no annealing treatment is involved. Thus the final product is a kind of mixture or composite rather than the coating or doping sample. However, we can find that even through the simple ball milling between Sb_2O_3 and bare sample, the composite can achieve a significant reduction of polarization increment with cycling and interface improvement. It is further conjectured that the existence of Sb_2O_3 may hinder the reaction between the charged cathode and the harmful decomposition product from electrolyte, and further avoid the adverse effect of electrolyte on highly oxidized cathode. According to this assumption, we tried to assemble the coin cell with different constructions, in which a thin layer of Sb_2O_3 was put on the anode surface or between cathode and separator. It is conceived that if the main function of Sb_2O_3 is to hinder the interaction between the decomposition product of electrolyte at the high voltage and the highly oxidized cathode, it can play some positive effect no matter whether it has contact with cathode or not.

In Fig. 8, the role of Sb_2O_3 is investigated by comparing the rate property of four different cells. In the cell named "Sb_2O_3 attached to separator", a thin layer of Sb_2O_3 has been placed between bare $LiNi_{1/3}Co_{1/3}Mn_{1/3}O_2$ cathode and Celgard 2300 separator. While in the cell named "Sb_2O_3 attached to anode", a thin layer of Sb_2O_3 has been placed on the surface of lithium anode. The rate performance of the bare $LiNi_{1/3}Co_{1/3}Mn_{1/3}O_2$ cathode and $Sb_2O_3/LiNi_{1/3}Co_{1/3}Mn_{1/3}O_2$ cathode is also displayed together in Fig. 8. It is amazing to find that "Sb_2O_3 attached to separator" and "Sb_2O_3 attached to anode" cells both exhibit similar rate performances to the cell with $Sb_2O_3/LiNi_{1/3}Co_{1/3}Mn_{1/3}O_2$ composite cathode. The results prove our assumption that the role of Sb_2O_3 is to hinder the harmful reaction between electrolyte and cathode during the charge/discharge process and help to stabilize the interface. As the Sb_2O_3 layer on anode surface may cause some unwanted deposition of the alien metal in a practical battery due to the low potential on anode side, we think using Sb_2O_3-coated separator can achieve the positive effect in a practical battery. Recent work on Al_2O_3-coated separator already proved the viability of this concept [24]. Further work is in progress in our lab.

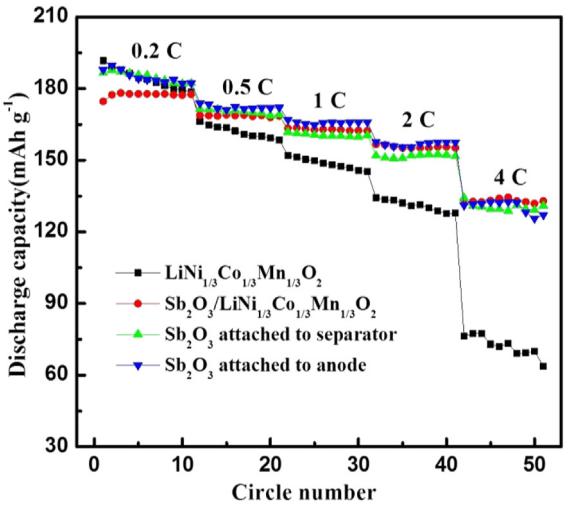

Fig. 8. Comparison of the rate performance of the cells with different configurations between 3.0 V and 4.6 V.

4. Conclusion

In this paper, two Sb_2O_3-modified layered $LiMO_2$ (M = Ni, Co and Mn) materials have been prepared by rheological phase method and ball-milling post-treatment. XRD measurements prove the existence of Sb_2O_3 in the composite. Meanwhile, SEM and TEM reveal that the Sb_2O_3 particles adhere to the surface of $LiMO_2$ active materials. Due to the presence of Sb_2O_3, $Sb_2O_3/LiMO_2$ ($LiMO_2 = LiNi_{1/3}Co_{1/3}Mn_{1/3}O_2$ or $LiNi_{0.4}Co_{0.2}Mn_{0.4}O_2$) shows greatly improved cycling stability and rate capability. AC impedance measurement shows that the smaller R_{ct} and/or R_f value in $Sb_2O_3/LiMO_2$ electrodes is the main reason for the improved electrochemical property. Because of the stabilized interface, $Sb_2O_3/LiMO_2$ electrodes also show significantly enhanced thermal safety. Further experiments prove that Sb_2O_3 layer placed either on lithium anode or between separator and cathode can bring similar positive effect on layered $LiMO_2$ electrode. The result inspires us to fabricate Sb_2O_3-coated separator and that work is in progress in our group.

Acknowledgements

Authors would express their sincere thanks to the Nature Science Foundation of China (No. 21073138, 21273168, 21233004) for the financial support.

References

[1] J. Liu, J.-G. Zhang, Z. Yang, J.P. Lemmon, C. Imhoff, G.L. Graff, L. Li, J. Hu, C. Wang, J. Xiao, G. Xia, V.V. Viswanathan, S. Baskaran, V. Sprenkle, X. Li, Y. Shao, B. Schwenzer, Adv. Funct. Mater. 23 (2013) 929–946.
[2] B. Xu, D. Qian, Z. Wang, Y.S. Meng, Mater. Sci. Eng. R 73 (2012) 51–65.
[3] T. Ohzuku, Y. Makimura, Chem. Lett. 7 (2001) 642–643.
[4] N. Igawa, T. Taguchi, H. Fukazawa, H. Yamauchi, W. Utsumi, J. Am. Ceram. Soc. 93 (2010) 2144–2146.
[5] W.-S. Yoon, M. Balasubramanian, K.Y. Chung, X.-Q. Yang, J. McBreen, C.P. Grey, D.A. Fischer, J. Am. Chem. Soc. 127 (2005) 17479–17487.
[6] J. Zheng, J.-J. Chen, X. Jia, J. Song, C. Wang, M.-S. Zheng, Q.-F. Dong, J. Electrochem. Soc. 157 (2010) 702–706.
[7] Y.-K. Sun, B.-R. Lee, H.-J. Noh, H. Wu, S.-T. Myung, K. Amine, J. Mater. Chem. 21 (2011) 10108–10112.
[8] K.M. Shaju, G.V.S. Rao, B.V.R. Chowdari, Electrochim. Acta 48 (2002) 145–151.
[9] P.-Y. Liao, J.-G. Duh, J.-F. Lee, J. Power Sources 189 (2009) 9–15.
[10] M. Wang, Y. Chen, F. Wu, Y. Su, L. Chen, D. Wang, Electrochim. Acta 55 (2010) 8815–8820.
[11] J. Li, X. He, R. Zhao, C. Wan, C. Jiang, D. Xia, S. Zhang, J. Power Sources 158 (2006) 524–528.
[12] K.C. Kam, M.M. Doeff, J. Mater. Chem. 21 (2011) 9991–9993.
[13] H.J. Kweon, G.B. Kim, D.G. Park, K.R. Patent Appl. 1998/0012005.
[14] J.-P. Yu, X.-H. Hu, H. Zhan, Y.-H. Zhou, J. Power Sources 189 (2009) 697–701.
[15] B. Lin, Z. Wen, X. Wang, Y. Liu, J. Solid State Electrochem. 14 (2010) 1807–1811.
[16] F. Wu, M. Wang, Y. Su, L. Bao, S. Chen, Electrochim. Acta 54 (2009) 6803–6807.
[17] J. Cho, T.-J. Kim, J. Kim, M. Noh, B. Park, J. Electrochem. Soc. 151 (2004) A1899–A1904.
[18] S.H. Yun, K.-S. Park, Y.J. Park, J. Power Sources 195 (2010) 6108–6115.
[19] H.G. Song, K.-S. Park, Y.J. Park, Solid State Ionics 225 (2012) 532–537.
[20] Y. Huang, J. Chen, J. Ni, H. Zhou, X. Zhang, J. Power Sources 188 (2009) 538–545.
[21] Y.-K. Sun, S.-T. Myung, M.-H. Kim, J. Prakash, K. Amine, J. Am. Chem. Soc. 127 (2005) 13411–13418.
[22] J.-W. Wen, D.-W. Zhang, Y.-C. Teng, C.-H. Chen, Y. Xiong, Electrochim. Acta 55 (2010) 2306–2310.
[23] D. Aurbach, B. Markovsky, A. Rodkin, E. Levi, Y.S. Cohen, H.-J. Kim, M. Schmidt, Electrochim. Acta 47 (2002) 4291–4306.
[24] Y.S. Jung, A.S. Cavanagh, L. Gedvilas, N.E. Widjonarko, I.D. Scott, S.-H. Lee, G.-H. Kim, S.M. George, A.C. Dillon, Adv. Energy Mater. 2 (2012) 1022–1027.